Ecology, 90(7), 2009, pp. 1971–1980

Modeling utilization distributions in space and time

Kim A. Keating[1,3] and Steve Cherry[2]

[1]*U.S. Geological Survey, Forestry Sciences Laboratory, Montana State University, Bozeman, Montana 59717 USA*
[2]*Department of Mathematical Sciences, Montana State University, Bozeman, Montana 59717 USA*

Abstract. W. Van Winkle defined the utilization distribution (UD) as a probability density that gives an animal's relative frequency of occurrence in a two-dimensional (x, y) plane. We extend Van Winkle's work by redefining the UD as the relative frequency distribution of an animal's occurrence in all four dimensions of space and time. We then describe a product kernel model estimation method, devising a novel kernel from the wrapped Cauchy distribution to handle circularly distributed temporal covariates, such as day of year. Using Monte Carlo simulations of animal movements in space and time, we assess estimator performance. Although not unbiased, the product kernel method yields models highly correlated (Pearson's $r = 0.975$) with true probabilities of occurrence and successfully captures temporal variations in density of occurrence. In an empirical example, we estimate the expected UD in three dimensions (x, y, and t) for animals belonging to each of two distinct bighorn sheep (*Ovis canadensis*) social groups in Glacier National Park, Montana, USA. Results show the method can yield ecologically informative models that successfully depict temporal variations in density of occurrence for a seasonally migratory species. Some implications of this new approach to UD modeling are discussed.

Key words: bighorn sheep; Glacier National Park, Montana, USA; home range; kernel density estimation; Metropolis-Hastings algorithm; nonparametric; Ovis canadensis; *product kernel estimator.*

Introduction

Van Winkle (1975:118) envisioned the utilization distribution (UD) "as the two-dimensional relative frequency distribution for the points of location of an animal over a period of time." His definition has contributed greatly to the contemporary notion of the home range as a probability density surface projected onto a two-dimensional (x, y) plane. It also has seeded important progress in home range modeling, as evidenced by numerous subsequent efforts to devise, adapt, or refine methods for estimating two-dimensional frequency distributions (Don and Rennolls 1983, Worton 1989, Seaman and Powell 1996, Getz and Wilmers 2004, Hemson et al. 2005, Hines et al. 2005, Börger et al. 2006, Horne and Garton 2006, Fieberg 2007*a*, *b*, Moser and Garton 2007) and by the innumerable studies applying such methods. Nonetheless, Van Winkle's (1975) definition of the UD lacks generality.

Although the UD concept is entrenched in the ecological literature as a strictly two-dimensional phenomenon, animal frequency distributions clearly occupy at least four dimensions. Van Winkle (1975:118) acknowledged the existence of three of these, stating that "[i]f the habitat is represented by a two-dimensional (X, Y) surface, the movements of an animal over time may be represented by a path in 3-space, the third dimension being time." He then effectively integrated time out of his model to gain a simplified two-dimensional framework for comparing modeling methods. By limiting the UD to the (x, y) plane, however, one implicitly assumes that temporal and elevation coordinates carry no ecologically important information. This assumption may be appropriate for studies such as Van Winkle's (1975), but in general, information associated with time and elevation can be critical to ecological understanding. For example, Spencer et al. (1991) found that spatial and temporal distributions of pelagic organisms (specifically, their elevations within the water column at different times of the day) can alter trophic interactions, transforming a predator–prey relationship into one of interspecific competition. Thus, we argue for a more general definition of the UD, one that fully encompasses the four dimensions of space and time.

We extend Van Winkle's (1975) work by defining the UD as the relative frequency distribution of an animal's occurrence in space and time. Our definition acknowledges that animal occurrence is distributed in four dimensions with coordinates (x, y, z, t), where z and t are, respectively, elevation and time. Our definition allows for various special cases. For example, in our notation Vokoun's (2003) one-dimensional model is designated UD_x, Van Winkle's (1975) two-dimensional case is $UD_{x,y}$, and Rader and Krockenberger's (2006) three-dimensional spatial model is $UD_{x,y,z}$. Other special cases are possible. In this paper, we emphasize UD models for strictly terrestrial species, where z is uniquely

Manuscript received 13 June 2008; revised 26 September 2008; accepted 20 October 2008. Corresponding Editor: M. C. Wimberly.

[3] E-mail: kkeating@usgs.gov

specified by (x, y) and so conveys no additional information. Thus, we omit z from our models and consider the three-dimensional case $UD_{x,y,t}$. We begin by describing a product kernel model estimation procedure. To handle circularly distributed covariates (e.g., day of year) we devise a novel kernel based on the wrapped Cauchy distribution. We then model movements of a seasonally migratory animal to explore estimator performance in a situation in which the true $UD_{x,y,t}$ is known, focusing especially on the ability to model temporal variations in density of occurrence. Finally, we give an empirical example, estimating the expected $UD_{x,y,t}$ for animals belonging to two distinct bighorn sheep (*Ovis canadensis*) social groups in Glacier National Park, Montana, USA.

Product Kernel Estimation

Product kernel algorithm

Our description of the product kernel method follows from Silverman (1986) and Scott (1992). We begin with the univariate case, in which an animal's location is measured along a single c-axis. For example, location might be measured as distance from the mouth of a stream, as in Vokoun (2003). The problem is to estimate ($\widehat{UD}_c$) the value of the UD at a user-selected location, c, given the vector $\mathbf{u}' = [u_1, u_2, \ldots, u_n]$ of locations recorded for a random sample of $i = 1, \ldots, n$ occurrences of the study animal. We might choose, for example, to estimate the UD of an individual fish at a point $c = 2$ km from the stream's mouth, given a random sample of n occurrences of that fish, where the location of each occurrence also is measured as distance from the stream's mouth. The kernel density method calculates $\widehat{UD}_c$ as the weighted average of the n observed values in $\mathbf{u}$; the closer an observed value is to the c value at which we wish to estimate density, the more weight it receives. This is achieved by centering a weighting function (kernel) over each observation $u_1, \ldots, u_n$, yielding a series of what Silverman (1986:15) refers to as "bumps." Estimated density is proportional to the sum of those bumps at c. This method is nonparametric, making no assumption about the underlying form of the density. In our notation, it is commonly formulated as follows (Silverman 1986, Scott 1992):

$$\widehat{UD}_c = \frac{1}{nh}\sum_{i=1}^{n} K\left(\frac{c - u_i}{h}\right)$$

where h determines the width of the bumps (bandwidth) and K is the kernel weighting function. For convenience, we also use the notation $v_i = (c - u_i)/h$.

In the multivariate case, in which the location of a point is specified in d dimensions by the coordinates $\mathbf{c}' = (c_i, \ldots, c_d)$, the problem is to estimate the UD at each user-selected point of interest, given the coordinate vectors $\mathbf{u}_i' = (u_{i,1}, \ldots, u_{i,d})$ recorded for our n randomly sampled occurrences of the animal. To extend the kernel method to d dimensions, we use the following product kernel estimator (Silverman 1986, Scott 1992):

$$\widehat{UD}_{\mathbf{c}} = \frac{1}{nh_1h_2\cdots h_d}\sum_{i=1}^{n}\left[\prod_{j=1}^{d} K_j\left(\frac{c_j - u_{i,j}}{h_j}\right)\right]. \quad (1)$$

Eq. 1 yields estimates of density of use within the d-dimensional parameter space, making no assumption about the underlying form of the density. In the applications we consider, $d \leq 4$ and $\mathbf{c} = (x, y, z, t)$ or a subset thereof.

Kernel choice

In general, the kernel function K/h must be a valid probability density function (pdf) to ensure that $\widehat{UD}_{\mathbf{c}}$ is a valid probability density estimate. Because the kernel estimator's performance is otherwise robust to the particular form chosen for K (Silverman 1986, Scott 1992), we focused on choosing computationally convenient kernels appropriate to our data types. For the spatial coordinates x, y, and z we used the biweight kernel:

$$K(v_i) = \begin{cases} \frac{15}{16}\left(1 - v_i^2\right)^2 & \text{for } |v_i| < 1 \\ 0 & \text{otherwise} \end{cases}$$

due to its high efficiency (Silverman 1986:43, Scott 1992:140) and because Scott (1992:146–149) provides formulations for biweight boundary kernels, which we use in a separate but related study. The biweight kernel is appropriate for continuous linear covariates with support on the interval [$-\infty$, ∞]. It is applicable to temporal covariates when treating time as a continuous linear variable. In our applications, however, we record time as day of year (transformed to radians), which is a continuous circular covariate with support on the interval [$-\pi$, π] radians. To handle circular covariates, we devise a kernel from the pdf for the wrapped Cauchy distribution (Batschelet 1981:282, Eq. 15.4.2):

$$K(v_i) = \frac{h\left[1 - (1-h)^2\right]}{2\pi[1 + (1-h)^2 - 2(1-h)\cos(v_i h)]} \quad (2)$$

$0 < h \leq 1$. The quantity $(1 - h)$ replaces mean vector length in the wrapped Cauchy equation and determines concentration of probability for this pdf. When $h = 1$, Eq. 2 yields a uniform circular distribution. As h becomes small, probability becomes increasingly concentrated.

Bandwidth selection

Bandwidth selection is the main problem in applying kernel density estimation. In general, choosing bandwidths that are too small yields noisy estimates with spurious structure, while choosing bandwidths that are too large yields oversmoothed estimates that obscure important structure. To better ensure objective results,

we use an objective bandwidth selection procedure. Readers are reminded, however, that "[t]he importance of choosing optimal bandwidth is easily overstated" (Scott 1992:161) and that it may sometimes be appropriate to choose bandwidths subjectively (Silverman 1986:44, Scott 1992:161).

For multivariate problems, Zhang et al. (2006) suggest a Bayesian approach for choosing **h**, using a likelihood cross-validation criterion. We use Zhang et al.'s (2006) method for determining a diagonal bandwidth matrix, which is equivalent to estimating the vector $\mathbf{h}' = (h_1, \ldots, h_d)$ for the product kernel estimator of Eq. 1. Treating **h** as a d-dimensional parameter vector, Zhang et al. (2006) assume the prior density of each component of **h** is as follows (up to a normalizing constant):

$$\pi(h_j|\lambda) \propto \frac{1}{1+\lambda h_j^2}$$

for $j = (1, 2, \ldots, d)$, where λ is a hyperparameter governing density shape. They further observe that, conditional on **h** and **u**, an estimate of the sampling distribution is given by the leave-one-out kernel density estimate:

$$\widehat{\mathrm{UD}}_{\mathbf{c}_k} = \frac{1}{(n-1)h_1h_2\cdots h_d}\sum_{\substack{i=1\\ i\neq k}}^{n}\left[\prod_{j=1}^{d} K_j\left(\frac{c_{k,j}-u_{i,j}}{h_j}\right)\right]. \quad (3)$$

Note that, here, the c_k are the leave-one-out values drawn from the pool of n randomly sampled instances of occurrence, rather than user-specified points of interest as in Eq. 1. From Bayes' Rule, the posterior distribution of **h** is as follows (up to a normalizing constant):

$$\pi(\mathbf{h}|\mathbf{u}_1,\ldots,\mathbf{u}_n) \propto \left(\prod_{j=1}^{d}\frac{1}{1+\lambda h_j^2}\right)\left(\prod_{k=1}^{n}\widehat{\mathrm{UD}}_{\mathbf{c}_k}\right). \quad (4)$$

Following Zhang et al. (2006), we set $\lambda = 1$ and use a Metropolis-Hastings algorithm (Gelman et al. 2004:289 et seq.) to sample from $\pi(\mathbf{h}\,|\,\mathbf{u}_1, \ldots, \mathbf{u}_n)$. Our implementation proceeds through m iterations, as follows:

1) Calculate starting bandwidth values, $h_1^0, h_2^0, \ldots, h_d^0$.
2) For iterations $w = 1, 2, \ldots, m$
   a) for dimensions $j = 1, 2, \ldots, d$
      i) draw a proposal bandwidth value, h_j^*, from a Gaussian proposal distribution with mean h_j^{w-1} and standard deviation σ_j,
      ii) using Eq. 4, calculate the ratio of densities,

$$r = \frac{\pi(\mathbf{h}^*|\mathbf{u}_1,\ldots,\mathbf{u}_n)}{\pi(\mathbf{h}^{w-1}|\mathbf{u}_1,\ldots,\mathbf{u}_n)}$$

where $\mathbf{h}^*$ is the bandwidth vector that includes the new proposal value h_j^* and $\mathbf{h}^{w-1}$ is the vector containing h_j^{w-1},

      iii) draw a uniform random number in the range [0, 1], then set

$$h_j^w = \begin{cases} h_j^* & \text{with probability } \min(r,1) \\ h_j^{w-1} & \text{otherwise.} \end{cases} \quad (5)$$

This process yields a sample whose density converges to $\pi(\mathbf{h}\,|\,\mathbf{u}_1, \ldots, \mathbf{u}_n)$ as $m \to \infty$, but rates of convergence can vary with starting values. To focus the process on the region of parameter space in which values of h_j^w are associated with nontrivial probability densities, it is usual to employ an initial burn-in period of some large number of iterations. Details regarding starting bandwidths, choice of σ_j values, and numbers of total and burn-in iterations for our specific applications are given below. Code to implement the Metropolis-Hastings algorithm (see Supplement) was written and compiled using Intel Visual Fortran version 10.0 for Windows (Intel, Santa Clara, California, USA).

Monte Carlo Simulations

Using Monte Carlo simulations, we evaluated whether the product kernel method yields reasonable estimates of density of occurrence for a seasonally migratory animal. Our simulations used a 100×100 cell model landscape in which the unit of distance for the x and y axes was equal to the cell width. For each cell, we calculated elevation (z) as a bivariate normal density with mean $\mu_x = \mu_y = 50$ and standard deviation $\mathrm{SD}_x = \mathrm{SD}_y = 15$, scaled by an arbitrary constant (10^7). We calculated aspect (θ, in radians) as the direction from the center of the landscape to the center of each cell.

Probability of occurrence for our model animal varied with z, θ, and t. Density of occurrence with respect to z (Appendix A) was beta-distributed (Johnson et al. 1995) as

$$f_z(t) = \frac{1}{B(a_t,b_t)}\left(\frac{z-z_{\min}}{z_{\max}-z_{\min}}\right)^{a_t-1}\left(1-\frac{z-z_{\min}}{z_{\max}-z_{\min}}\right)^{b_t-1} \quad (6)$$

where $z_{\min} = 0.132$ and $z_{\max} = 7063.085$ were, respectively, the minimum and maximum elevations observed in our model landscape and $B(a_t, b_t)$ is the beta function with parameters (a_t, b_t) that varied with time, measured as day of year (DOY). To induce seasonally migratory behavior with respect to elevation, we calculated (a_t, b_t) as

$$a_t = \frac{1}{2}\left\{a_{\min} + \cos\left[t\left(\frac{2\pi}{365}\right)+\frac{\pi}{2}+1\right](a_{\min}-a_{\max})\right\}$$

$$b_t = \frac{1}{2}\left\{b_{\min} + \sin\left[t\left(\frac{2\pi}{365}\right)+1\right](b_{\min}-b_{\max})\right\} \quad (7)$$

where $a_{\min} = b_{\min} = 2$, and $a_{\max} = b_{\max} = 6$. Minimum and maximum values of (a_t, b_t) were chosen so that peak

probabilities of occurrence cycled between high and low elevations during the year (Appendix A).

We let density of occurrence with respect to aspect (Appendix B) be circularly skew distributed (Batschelet 1981:286, Eq. 15.6.4) as

$$g_\theta(t) = \frac{1}{2\pi} + \frac{\gamma}{2\pi}\cos[\theta - \kappa_t + \tau\cos(\theta - \kappa_t)] \qquad (8)$$

where θ is in radians, $-1 \leq \gamma \leq 1$ is a concentration parameter, τ determines skewness, and κ_t is a time-dependent location parameter. We set $\gamma = 0.95$ and $\tau = \pi/6$, but let the distribution's location vary with t according to $\kappa_t = 2\pi t/365$. Thus, the shape of the density distribution with respect to θ was constant, but the distribution's mode revolved during the year around the "mountain" of our model landscape (Appendix B).

Letting elevation and aspect be independent effects, we calculated probability of occurrence for each cell in our landscape on any particular DOY as

$$\mathrm{UD}(t) = \frac{f_z(t)g_\theta(t)}{\sum f_z(t)g_\theta(t)}. \qquad (9)$$

The summation in the denominator assures the necessary unit sum constraint in the discrete space of our model landscape.

Based on Eq. 9, we randomly allocated five locations per day among the cells in our landscape, recording the location (x, y) and time (t) of each. Repeating this procedure for each DOY ($t = 1, \ldots, 365$) gave a sample of $n = 1825$ locations per year, a sampling rate we chose as comparable to the observed rate in our empirical example below. Using these samples and the product kernel estimator (Eq. 1), we then estimated probability of occurrence for each cell and DOY ($\widehat{\mathrm{UD}}_{x,y,t}$). To determine bandwidths, we set starting values at $h_x^0 = h_y^0 = 5$ and $h_t^0 = 0.2$. Following a small amount of experimentation, we chose these values to avoid excessive convergence time and, thereby, limit the Metropolis-Hastings procedure to $m = 2000$ iterations, including a burn-in period of 500 iterations. Standard deviations of $\sigma_x = \sigma_y = 0.25$ and $\sigma_t = 0.05$ for the Gaussian proposal distributions were similarly chosen to achieve acceptance rates (Eq. 5) of approximately 0.25 ± 0.10. Repeating our sampling procedure 50 times, we calculated the mean estimate ($\overline{\widehat{\mathrm{UD}}}_{x,y,t}$) for each cell and DOY and visually compared these estimates with true $\mathrm{UD}_{x,y,t}$ values to assess estimator performance. Known and estimated probability densities for each DOY also were linked in video clips to allow visual comparison, show the time-continuous nature of both the true density of occurrence and the product kernel estimates, and illustrate the kinds of temporally dynamic visualization tools made possible by this method (Appendices C and D). Finally, for each DOY we drew five cells randomly with replacement from our model landscape and recorded $\mathrm{UD}_{x,y,t}$ and $\widehat{\mathrm{UD}}_{x,y,t}$ for each. Using this subsample, we calculated Pearson's r to assess the strength of the correlation between known and estimated values, and we plotted $\overline{\widehat{\mathrm{UD}}}_{x,y,t}$ on $\mathrm{UD}_{x,y,t}$ to identify biases.

Monte Carlo results indicated successful overall performance of the product kernel method, as evidenced by the strong correlation (Pearson's $r = 0.975$) between $\mathrm{UD}_{x,y,t}$ and $\widehat{\mathrm{UD}}_{x,y,t}$ values. Day-by-day comparisons further showed that the product kernel estimator gave UD models that successfully capture both spatial and temporal variations in density of occurrence. For example, $\overline{\widehat{\mathrm{UD}}}_{x,y,t}$ values clearly and appropriately showed peak concentrations of use at high elevations and southwesterly aspects on approximately day 274 and use that was least concentrated on approximately day 94, when low elevations and northeasterly aspects were favored (Fig. 1). Full depictions of true and estimated UD values are available as animations (Appendices C and D). However, $\overline{\widehat{\mathrm{UD}}}_{x,y,t}$ values were not unbiased. Plotting $\overline{\widehat{\mathrm{UD}}}_{x,y,t}$ on $\mathrm{UD}_{x,y,t}$ for 1825 randomly selected (x, y, t) coordinates showed that very low UD values tended to be overestimated, whereas high values tended to be underestimated (Fig. 2). This result is consistent with the fact that kernel smoothing involves a bias–variance trade-off that is mediated by bandwidth (Silverman 1986:38–40, Fieberg 2007*b*). Because bandwidths in this study were chosen as a function of n, the observed biases are ultimately attributable to sample size effects.

Example: Modeling Utilization Distributions of Bighorn Sheep (*Ovis canadensis canadensis* Shaw) in Glacier National Park, Montana

To demonstrate our method, we modeled utilization distributions of Rocky Mountain bighorn sheep in Glacier National Park (GNP), Montana, USA. Twenty-one ewes were captured in the Many Glacier area of GNP during 2002–2005 using protocols approved by an Animal Care and Use Committee and were fit with Telonics radio collars (Telonics, Mesa, Arizona, USA) equipped with global positioning systems and automatic release mechanisms. The collars were programmed to record location once every 5 h and release after approximately one year. Collars recorded latitude and longitude, as well as date and time referenced to Greenwich Mean Time. Before analyses, location data were transformed to Universal Transverse Mercator coordinates using Corpscon version 5.11.08 (U.S. Army Corps of Engineers, Topographic Engineering Center, Alexandria, Virginia, USA). Time and date codes were converted to Mountain Standard Time, then to decimal DOY and, ultimately, to radians.

Our goal was to model expected UDs for animals belonging to different social groups. Bighorn sheep are gregarious and generally follow traditional movement patterns that are learned, being passed from one generation to the next (Geist 1971). Thus, they tend to form distinct social groups, especially among females. Our telemetry data revealed clear evidence of two ewe

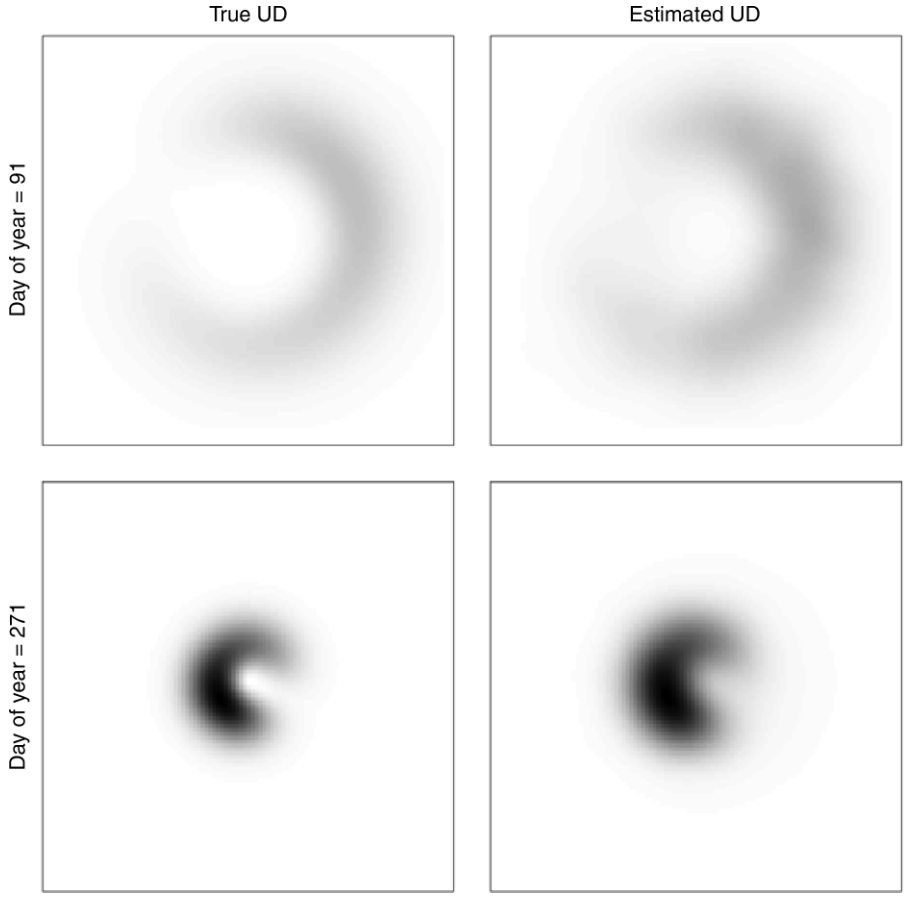

FIG. 1. Results of Monte Carlo simulations, comparing true vs. mean estimated density of use over the model landscape. The top row shows results for day of year (DOY) = 91, when low elevations and northeast aspects were preferred, resulting in relatively scattered animal use. The bottom row shows results for DOY = 271, when high elevations and southwest aspects were preferred, resulting in more concentrated use. In each graph, density is scaled from zero (white) to the highest value observed over the entire year (black). Upper bounds used to plot the true and mean estimated densities were 2.758×10^{-3} and 1.793×10^{-3}, respectively.

social groups in the Many Glacier area, the Sheep Curve (SC) and Iceberg–Ptarmigan (IP) groups. To model expected UDs of animals belonging to these groups, we first assigned each study animal to a social group based on visual examination of the telemetry data. Clear separation in annual ranges of the groups made unambiguous assignments possible. We then modeled $UD_{x,y,t}$ for each individual. Using Scott's rule in d dimensions (Scott 1992:152, Eq. 6.42), we calculated starting bandwidth values h_x^0 and h_y^0 as

$$h_j^0 = \hat{\sigma}_j n^{-1/(d+4)}$$

where $\hat{\sigma}_j$ is the estimated standard deviation calculated from the n recorded coordinates for the jth dimension. Following limited experimentation, we set $h_t^0 = 0.019$. Proposal distributions for all dimensions were Gaussian. For the x and y dimensions, standard deviations for the proposal distributions were initially set equal to $h_j^0/100$. For the t dimension, the standard deviation of the proposal distribution was initially set at 0.01. For proposal distributions for all dimensions, we used an iterative procedure to choose final standard deviations that achieved acceptance rates for proposal values (Eq. 5) of 0.25 ± 0.10. Proposal values were constrained to ensure $h_x^* > 0$ and $h_y^* > 0$, and $0 < h_t^* \leq 1$. For each animal, our Metropolis-Hastings procedure used 2000 iterations, including 1000 burn-in iterations. The value of $\mathbf{h}$ used to obtain final product kernel density estimates was calculated as the median of the 1000 post-burn-in values of $\mathbf{h}^w$. For each DOY, we calculated the expected UD of animals belonging to each group by averaging estimated UDs over all animals sampled from that group. Results were then standardized to ensure estimated mean UDs summed to 1 over all cells for each DOY. Finally, estimated UDs for each DOY were linked in an animation to show the time-continuous nature of the product kernel estimates and to illustrate the kinds of temporally dynamic visualization tools made possible by this method (Appendix E).

We recorded 28 134 relocations of our study animals, including 18 781 relocations of 15 ewes from the SC group and 9353 relocations of six ewes from the IP group. Mean sample size over all 21 animals was 1339.7

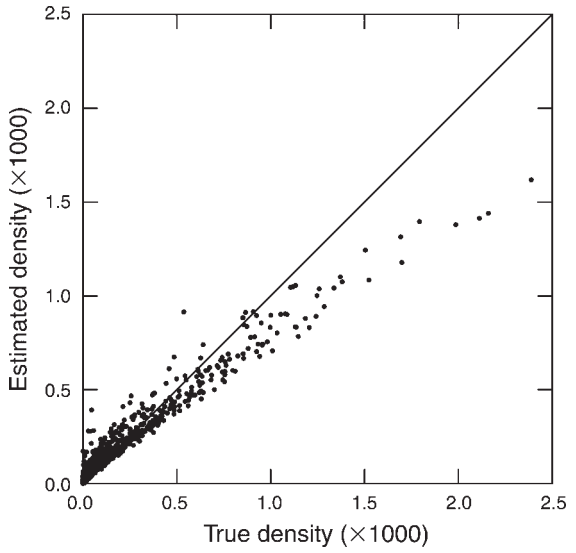

FIG. 2. Plot of mean estimated density of use on true density for 1825 randomly selected (x, y, t) coordinates. The solid line shows the ideal relationship between true and estimated values. Low values tended to be overestimated, and high values were underestimated.

relocations (SD = 470.4, range = 346–2063). Median bandwidths (±SE) chosen via the Bayesian method of Zhang et al. (2006) averaged 0.537 (±0.006) km, 0.715 (±0.006) km, and 0.0072 (±0.0002) for the x, y, and t coordinates, respectively. Bandwidths for t were quite narrow. On average, they placed 96% of the kernel weight in a window of ±7 d and 75% of the weight in a window of ±1 d. Thus, we expect that, given our sample sizes, the product kernel method should capture relatively fine-scale temporal variations in density of occurrence. Mean UD models confirmed our expectation. For example, models clearly showed shifts in density of use associated with lambing, movements to salt licks, the late-summer dry season, and fall rut (Fig. 3). See Appendix E for a complete depiction of seasonal changes in density of occurrence.

DISCUSSION

Reviewing nearly a century of animal home range literature, Laver and Kelly (2008) found few studies that consider the influence of elevation or time on an animal's UD and none offering a unified framework for integrating elevation and temporal information with information about an animal's location in the (x, y) plane. They conclude there is "much potential" for "development of home range theory to incorporate the dimension of time, and eventually, time-volume considerations" (Laver and Kelly 2008:293). We agree. Van Winkle's (1975) two-dimensional definition of the UD, a cornerstone of home range studies for over 30 years, was devised as a simplified framework to compare alternative home range estimators. Limiting the UD to only two dimensions was a practical choice. Because he compared only one- and two-dimensional models, Van Winkle (1975) did not need a more general framework. Also, limitations in statistical theory and computing power at that time would have encouraged simplification. We submit, however, that it is time to revisit the two-dimensional paradigm, recognize that important information may be sacrificed by discarding elevation and temporal data, and consider whether a more general model might, in many cases, provide greater ecological insight. We argue for defining the UD as the relative frequency distribution of an animal's occurrence in space and time. By generalizing the UD concept to encompass all four dimensions of space and time, we explicitly recognize the potential importance of information associated with each spatial and temporal coordinate (x, y, z, and t) and caution that no such information should be discarded without conscious deliberation.

Given this general framework, it is easy to see that kernel density estimation, the prevalent method for modeling two-dimensional UDs (Laver and Kelly 2008), is readily applicable for modeling higher dimensional UDs. Indeed, Scott (1992:24, 26) describes an analogous application using spatial and temporal coordinates of seismic events near Mount St. Helens. Kernel density estimation exhibits some distinct advantages in this setting. It permits direct use of all common data types (including circular covariates, such as day of year) without resorting to problematic transformations. It also automatically accounts for interactions among covariates. These traits are especially important when assessing the effect of time on the UD. At first glance, time is an unusual covariate to include in a UD model because (barring death) density of occurrence is necessarily uniform with respect to time. Thus, the special one-dimensional case UD_t is of little interest because, unless the study animal dies or sampling of locations is biased over time, it would necessarily yield only a uniform distribution. However, considerable information about an animal's UD may reside in the interactions between time and the spatial coordinates x, y, and z, e.g., in the case of migratory or circadian movements, in which probability of occurrence varies systematically with day of year or time of day. Such an effect is evident in our Monte Carlo simulations and in our empirical example, where we show that the product kernel method can be used to estimate temporally dynamic UDs, thereby incorporating seasonally migratory behavior directly into the UD model.

Time also is an unusual covariate because it can be treated as either continuous linear or continuous circular, depending on the question being addressed. For example, if one is modeling changes in density of occurrence over a period of years, time should be treated as continuous linear, but when modeling seasonally migratory behavior it is appropriate to treat time as continuous circular. This duality poses a special problem. Development of kernel density methods has

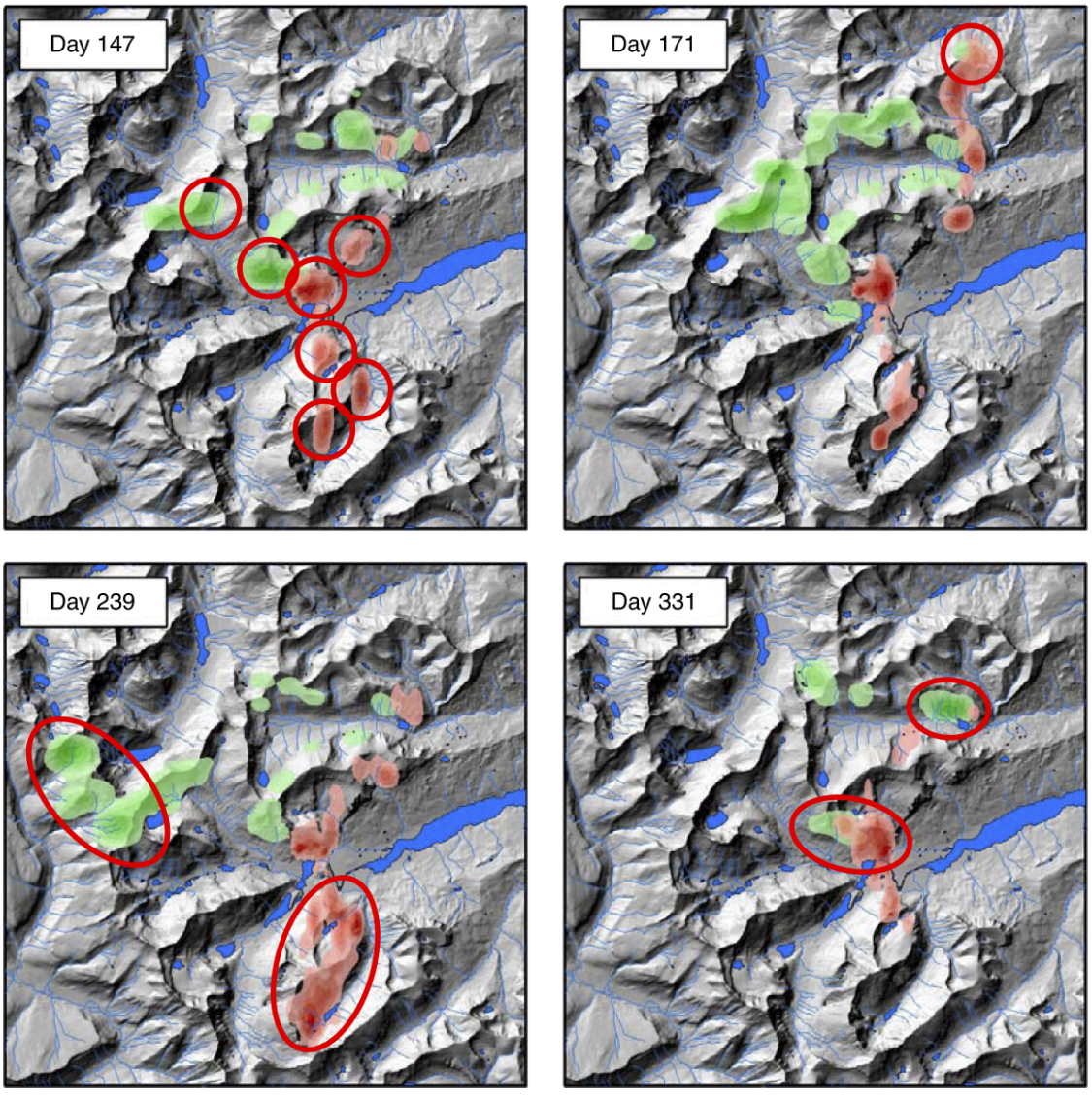

FIG. 3. Modeled utilization distributions (UDs) for selected days of the year, showing mean estimated density of occurrence for 15 bighorn ewes belonging to the Sheep Curve group (red) and six belonging to the Iceberg–Ptarmigan group (green) in Glacier National Park, Montana, USA. From darkest to lightest, variations in shading show the 10th, 30th, 50th, 70th, and 90th percentiles of the kernel density estimates. Model UDs for these days illustrate the ability to depict seasonal changes in concentrations of use as animals move to known lambing areas (red circles, day 147), a major salt lick (red circle, day 171), late-summer habitat (red ovals, day 239), and rutting grounds (red ovals, day 331). See Appendix E for an animation showing the complete modeled relationship between estimated density of use and day of year.

focused predominately on continuous linear variables (Silverman 1986, Scott 1992), thus numerous kernels are available to studies treating time as continuous linear. When treating time as continuous circular, however, a fundamentally different kernel, specific to this data type, is needed to ensure observations are weighted appropriately. For example, when estimating density of occurrence on day 365, observations of occurrence on day 1 merit greater weight than observations on day 360. Because our literature search revealed no kernel designed for circularly distributed data, we adapted the wrapped Cauchy pdf (Batschelet 1981). Our approach properly ensures (Silverman 1986:13–14) that the resulting kernel is everywhere non-negative and integrates to 1 over the range $[-\pi, \pi]$ radians. Results of both our Monte Carlo simulations and empirical example confirm the usefulness of the wrapped Cauchy kernel for incorporating continuous circular covariates into kernel density models. We note, however, that the wrapped Cauchy is not the only distribution that might be employed. Theoretically, pdfs for other symmetric, circular distributions, e.g., the von Mises, wrapped normal, or cosine distributions (Batschelet 1981:275 et seq.), might also be used. Because density estimates

involving continuous linear covariates are generally robust to kernel choice (Scott 1992:133), we expect that estimates involving circular covariates should be similarly robust. We use the wrapped Cauchy because it is computationally straightforward and offers support over the range $0 \leq h < 1$ and because we experienced numerical problems with the von Mises pdf.

Incorporating elevation and time directly into UD models eliminates the need to bin data into discrete categories of elevation (e.g., Rader and Krockenberger 2006) or time, predicated on subjective decisions about where the boundaries of those categories occur. For example, when developing seasonal models it is common to begin with subjective decisions about when a given season begins and ends. By including time directly in the model as a continuous circular covariate, such subjective decisions are unnecessary. Indeed, the resulting models may challenge traditional notions about whether seasonal movements can be reliably partitioned into discrete periods. Geist (1971:63, 75) concludes that bighorn ewes in Banff National Park, Canada, may have up to four distinct seasonal ranges, winter, late winter/spring, summer, and lambing, and indicates that long-distance movements among them proceed in a rather orderly fashion, with ewes moving to winter range in late September–early October, to late winter/spring range in late March and April, and to lambing areas, then on to summer range in late May, June, and early July. In contrast to this orthodox characterization of bighorn seasonal movement patterns, our models paint a more fluid picture (Appendix E). Ewes in our study used multiple winter and late winter/spring ranges, moving freely among them during both periods; salt licks were used most often during late June–early July, but might be visited almost any time during the year; and during summer, although use tended to be concentrated in certain areas, individual ewes repeatedly traversed the full extent of their year-long range and might be found in any part of it at any time.

Overall, probability of occurrence for the bighorn sheep we studied varied with time according to predictable patterns, but it was not possible to neatly bin all habitat patches according to season of use. Instead, our models show bighorn UDs as stochastic in space and time, with probability of occurrence peaking in different locations during different seasons. These models also suggest a cautionary tale regarding more traditional seasonal models. Consider, for example, the situation in which winter range is of primary importance and the winter UD is estimated using only data gathered during the winter period. In our bighorn sheep example, this extends from approximately 15 November (DOY = 319) through 1 May (DOY = 121). Estimating the two-dimensional density $UD_{x,y}$ for this period would yield a model of density of occurrence averaged over the entire winter period. Model $UD_{x,y,t}$ clearly indicates, however, that use becomes more concentrated in late winter, with peak concentration confined to only a brief period (Appendix E; compare, for example, DOY = 43 vs. DOY = 121). This pattern has important implications for both monitoring and impact assessment. For example, observed changes in probability of occurrence within the winter season underscore the importance of the timing of annual monitoring surveys. Because concentration of use varies greatly within the winter season, minimizing inter-annual sampling variance (sensu White 2000) requires that annual surveys be conducted during periods when use is comparably concentrated, preferably during peak concentration. Knowing how probability of occurrence varies in space and time is, thus, important to optimizing monitoring efforts.

Temporal changes in the spatial distribution of use also have implications for impact assessment. For example, McDonald and McDonald (2002) suggest risks associated with alternative management scenarios can be assessed by comparing the area under a spatially explicit response surface (depicting relative probability of occurrence) before and after proposed management activities have been introduced. Incorporating a temporal component into this approach is relevant in two respects. First, magnitude of impact may depend critically on whether animal and human activities overlap in both space and time. Second, if human activity occurs in an area where animal use is hyper-concentrated for only a brief period, but impacts are evaluated using a response surface depicting mean relative probability of occurrence over a longer time period, then impacts may be underestimated.

Overall, we are encouraged by our results, which indicate that a generalized four-dimensional UD offers a useful conceptual framework for devising new approaches that incorporate information from elevation and temporal coordinates directly into UD models. They also demonstrate that product kernel density estimation provides a viable statistical method for estimating this higher dimensional model, one that is at least as good as the kernel methods now widely used for estimating two-dimensional UDs. Moreover, the wrapped Cauchy kernel extends the utility of kernel density estimation to include circularly distributed covariates. Our results, however, also point to the need for further work. In our bighorn study, for example, it seems likely that bandwidths calculated for individual bighorn sheep were too broad because we averaged results over multiple animals, thereby achieving an additional degree of smoothing outside the kernel estimation process. Guidance regarding bandwidth adjustment in this case would be helpful, but to our knowledge, the topic has not been addressed in the statistical literature. Such topics should provide fertile ground for further research.

Acknowledgments

The U.S. Geological Survey, Montana State University, the Glacier National Park Fund, and the U.S. National Park Service (NPS) supported this work. We thank NPS veterinarians J. Powers and M. Wild for assistance and advice and for

lending their field staff, V. Jameson and S. Ratchford, whose hard work and sacrificial knees are, likewise, appreciated. We benefited from an exceptional field crew that at various times included V. Boccadori, J. Brown, C. Dickenson, P. Lundberg, S. Schmitz, J. Shrum, and R. Yates. We also thank the many volunteers who contributed countless hours, and the GNP employees who aided our study, particularly J. Potter, S. Gniadek, R. Menicke, and the many rangers and maintenance workers at the Hudson Bay District Office. Former Park Superintendent S. Lewis lent a vital voice of support. Not least, we greatly appreciate the comments of D. W. Scott, M. L. Taper, J. Fieberg, and C. Calenge, who all helped improve this paper. Any use of trade, product, or firm names is for descriptive purposes only and does not imply endorsement by the U.S. Government.

Literature Cited

Batschelet, E. M. 1981. Circular statistics in biology. Academic Press, New York, New York, USA.

Börger, L., N. Franconi, G. de Michele, A. Gantz, F. Meschi, A. Manica, S. Lovari, and T. Coulson. 2006. Effects of sampling regime on the mean and variance of home range size estimates. Journal of Animal Ecology 75:1393–1405.

Don, B. A. C., and K. Rennolls. 1983. A home range model incorporating biological attraction points. Journal of Animal Ecology 52:69–81.

Fieberg, J. 2007*a*. Utilization distribution estimation using weighted kernel density estimators. Journal of Wildlife Management 71:1669–1675.

Fieberg, J. 2007*b*. Kernel density estimators of home range: smoothing and the autocorrelation red herring. Ecology 88: 1059–1066.

Geist, V. 1971. Mountain sheep: a study in behavior and evolution. University of Chicago Press, Chicago, Illinois, USA.

Gelman, A., J. B. Carlin, H. S. Stern, and D. B. Rubin. 2004. Bayesian data analysis. Second edition. Chapman and Hall/CRC, Boca Raton, Florida, USA.

Getz, W. M., and C. C. Wilmers. 2004. A local nearest-neighbor convex-hull construction of home ranges and utilization distributions. Ecography 27:489–505.

Hemson, G., P. Johnson, A. South, R. Kenward, R. Ripley, and D. MacDonald. 2005. Are kernels the mustard? Data from global positioning system (GPS) collars suggests problems for kernel home-range analyses with least-squares cross-validation. Journal of Animal Ecology 74:455–463.

Hines, W. G. S., R. J. O'Hara Hines, B. Pond, and M. E. Obbard. 2005. Allowing for redundancy and environmental effects in estimates of home range utilization distributions. Environmetrics 16:33–50.

Horne, J. S., and E. O. Garton. 2006. Likelihood cross-validation versus least squares cross-validation for choosing the smoothing parameter in kernel home-range analysis. Journal of Wildlife Management 70:641–648.

Johnson, N. L., S. Kotz, and N. Balakrishnan. 1995. Continuous univariate distributions. Volume 2. Second edition. John Wiley and Sons, New York, New York, USA.

Laver, P. N., and M. J. Kelly. 2008. A critical review of home range studies. Journal of Wildlife Management 72:290–298.

McDonald, T. L., and L. L. McDonald. 2002. A new ecological risk assessment procedure using resource selection models and geographic information systems. Wildlife Society Bulletin 30:1015–1021.

Moser, B. W., and E. O. Garton. 2007. Effects of telemetry location error on space-use estimate using a fixed-kernel density estimator. Journal of Wildlife Management 71:2421–2426.

Rader, R., and A. Krockenberger. 2006. Three-dimensional use of space by a tropical rainforest rodent, *Melomys cervinipes*, and its implications for foraging and home-range size. Wildlife Research 33:577–582.

Scott, D. W. 1992. Multivariate density estimation: theory, practice, and visualization. John Wiley and Sons, New York, New York, USA.

Seaman, D. E., and R. A. Powell. 1996. An evaluation of the accuracy of kernel density estimators for home range analysis. Ecology 77:2075–2085.

Silverman, B. W. 1986. Density estimation for statistics and data analysis. Chapman and Hall, New York, New York, USA.

Spencer, C. N., B. R. McClelland, and J. A. Stanford. 1991. Shrimp stocking, salmon collapse, and eagle displacement: cascading interaction in the food web of a large aquatic ecosystem. BioScience 41:14–21.

Van Winkle, W. 1975. Comparison of several probabilistic home-range models. Journal of Wildlife Management 39: 118–123.

Vokoun, J. C. 2003. Kernel density estimates of linear home ranges for stream fishes: advantages and data requirements. North American Journal of Fisheries Management 23:1020–1029.

White, G. C. 2000. Population viability analysis: data requirements and essential analyses. Pages 288–331 *in* L. Boitani and T. K. Fuller, editors. Research techniques in animal ecology: controversies and consequences. Columbia University Press, New York, New York, USA.

Worton, B. J. 1989. Kernel methods for estimating the utilization distribution in home-range studies. Ecology 70: 164–168.

Zhang, X., M. L. King, and R. J. Hyndman. 2006. A Bayesian approach to bandwidth selection for multivariate kernel density estimation. Computational Statistics and Data Analysis 50:3009–3031.

APPENDIX A

Video showing seasonal changes in simulated density of occurrence with respect to elevation, as per Eqs. 6 and 7 (*Ecological Archives* E090-136-A1).

APPENDIX B

Video showing seasonal changes in simulated density of occurrence with respect to aspect, as per Eq. 8 (*Ecological Archives* E090-136-A2).

APPENDIX C

Video showing the true utilization distribution, by day of year, for our Monte Carlo simulations, as per Eq. 9 (*Ecological Archives* E090-136-A3).

APPENDIX D

Video showing the mean estimated utilization distribution, by day of year, as calculated in our Monte Carlo simulations (*Ecological Archives* E090-136-A4).

APPENDIX E

Video showing estimated mean utilization distributions, by day of year, for bighorn ewes belonging to two social groups in Glacier National Park, Montana, USA (*Ecological Archives* E090-136-A5).

SUPPLEMENT

FORTRAN source code and dynamic link library files for implementing the Bayesian Markov Chain Monte Carlo (MCMC) bandwidth selection procedure used in this study (*Ecological Archives* E090-136-S1).